Coexistence of localization and itineracy of electrons in boron-doped diamond

Jifeng Yu,[1] Kai Ji,[2] Changqin Wu,[3] and Keiichiro Nasu[1,2]
[1]*Department of Materials Structure Science, The Graduate University for Advanced Studies, CREST JST, 1-1 Oho, Tsukuba, Ibaraki 305-0801, Japan*
[2]*Solid State Theory Division, Institute of Materials Structure Science, KEK, 1-1 Oho, Tsukuba, Ibaraki 305-0801, Japan*
[3]*Department of Physics, Fudan University, Shanghai 200433, China*
(Received 18 July 2007; revised manuscript received 4 October 2007; published 16 January 2008)

In order to clarify the coexistence of a Fermi edge and the steplike multiphonon structure, recently observed in the photoemission spectra (PES) of the boron-doped diamond, we apply a path-integral theory to calculate the PES, using the many-impurity Holstein model in a simple cubic lattice. Being lightly doped by boron as an acceptor, the diamond shows *p*-type character with an activation energy gap of about 0.37 eV. We find that, due to the electron-phonon coupling and the increase of the dopant concentration, the impurity band extends up to the top of valence band, and fills the gap gradually. The emergence of a clear Fermi edge is theoretically demonstrated, indicating the strong itineracy of electrons from one impurity atom to another through those intermediate carbon atoms. Simultaneously, the multiphonon satellite structure, a little below the Fermi level, is also theoretically reproduced in the doped site PES, denoting the localization of electrons through the coupling with Einstein phonons. Although we have used a simpler lattice structure than the real diamond one, our exploration of the coexistence of the two intrinsic properties of electrons: itineracy and localization, well agrees with the experimental findings.

DOI: 10.1103/PhysRevB.77.045207 PACS number(s): 71.23.−k, 78.20.Bh, 79.60.−i

I. INTRODUCTION

The boron-doped diamond (BDD) has become one of the most investigated materials since the remarkable discovery of its superconductivity (SC).[1] So far, most researches have been focusing on the very nature of phonon exchange mechanism,[2–5] which is still unclear though agreed to be responsible for the SC. It is well known that the pristine diamond is an insulator with a wide band gap (about 5.5 eV). Being lightly doped with boron, it shows *p*-type character with an activation energy gap of about 0.37 eV.[6] Accompanied with the superconducting phase, a semiconductor-metal transition occurs when the doping percentage is increased to a certain level.[7,8] Recently, Ishizaka *et al.*[9] declared the observation of a steplike multiphonon satellite structure in the valence band photoemission spectra (PES), approximately distributed periodically at 0.150 eV below the Fermi level, in addition to the emergence of a clear Fermi edge, indicating the phase transition mentioned above on increasing the dopant concentration. Compared with the scanned Raman scattering spectrum, this side structure is supposed to be attributed to the strong electron-phonon (e-ph) coupling by these authors.[9] Giustino *et al.*[10] also suggested that the 0.150 eV phonon plays an important role in the SC by the first-principles technique on the e-ph interaction of this material.

Meanwhile, this periodic satellite structure reminds one of its similarity to that of a localized electron model,[11] wherein the coupling between electrons and Einstein phonons characterizes the spectrum with discrete peaks of equal energy interval. Thus, it is natural to infer that the e-ph coupling has a close relation to this steplike structure as well. More importantly, the Fermi edge and the steplike structure are observed together, probably originating from the two basic properties of electrons: itineracy and localization. It also should be noted that the multiphonon structure appears not in the well-known gap function of the SC, but in the PES of the normal state. Hence, it seems quite unusual that this coexistence is detected so clearly and directly. Because of this puzzling behavior as well as a probable connection with the SC, the problem how this coexistence occurs, thus, turns out to be a great challenge for the theorists.

The coherent potential approximation (CPA),[12] being a standard method dealing with disordered systems, however, has some limitation in explaining the emergence of the Fermi edge. Because this theory tacitly assumes that the system remains uniform even after the doping, thus it ensures the presence of a certain Fermi edge at the very beginning, even in the low doping cases, while the conventional treatments, such as Midgal-Eliashberg theory, usually invoke perturbation theories, and have difficulty in dealing with this disordered system.

In this study, we use a path-integral theory[13] to survey the PES of BDD system. Correspondingly, we adopt a many-impurity Holstein model based on a simple cubic lattice. Actually, the Holstein model[14] has been widely used to discuss the e-ph coupling problems in various cases. For example, Ref. 16 studied the evolution of the PES with momentum in the one-dimensional and two-dimensional pure systems, at half-filling or non-half-filling. Using a Monte Carlo simulation with the traveling cluster approximation, Ref. 17 has investigated the effect of disorder on electronic transport property in strong e-ph coupling systems of three dimensions. There are also discussions about the dynamics of a single electron in the Holstein model with[18] or without[19] disorder. In the present paper, we shall be concerned with the doping and the e-ph coupling effects on the PES, especially the quantum character of phonons seen in the PES, rather than the classical one discussed in Ref. 17. To evaluate the PES, we shall apply the path-integral theory to take into account all kinds of e-ph scattering processes, which is technically impossible for the conventional perturbative methods.

The main purpose of this work is to investigate the e-ph coupling effect on the PES of a many-electron system, and theoretically clarify the aforementioned coexistence, then interpret the experimental findings in BDD. Here, it should be stressed that we focus only on the energy region very close to the Fermi level. Hence, we can use a simple cubic lattice instead of the real diamond one to describe the various valence band features, with no attention to the region far from the Fermi level. Unlike the conventional approaches such as CPA, the "doping" in this work is a random substitution, according to a certain given doping rate, to describe the disordered situation in BDD. It should be noted that, in the present problem, the so-called randomness and the doped electron number are closely related and changed simultaneously, being different from both a simple randomness problem and a simple doping problem.

II. MODEL AND METHODS

As mentioned, our model includes the following two properties. One is the disorder of the system that some atoms are replaced by the dopant in a certain ratio. The other is the coupling between electrons and Einstein phonons (site-localized lattice vibration), being the simplest description of e-ph interactions, usually called Holstein model. Its Hamiltonian ($\equiv H$) is given as ($\hbar=1$ throughout the work),

$$H = -t\sum_{\langle l,l'\rangle}\sum_{\sigma}(a_{l\sigma}^{\dagger}a_{l'\sigma}+a_{l'\sigma}^{\dagger}a_{l\sigma}) - \mu\sum_{l,\sigma}n_{l\sigma} + \Delta_e\sum_{l_0,\sigma}n_{l_0\sigma} + \frac{\omega_0}{2}\sum_{l}\left(-\frac{\partial^2}{\partial Q_l^2}+Q_l^2\right) - S\sum_{l,\sigma}Q_l(n_{l\sigma}-\bar{n}_l/2),$$

$$n_{l\sigma}\equiv a_{l\sigma}^{\dagger}a_{l\sigma},\quad \sigma=\alpha \text{ or } \beta, \tag{1}$$

where t is the hopping energy, set at $t=0.42$ eV in the simulations to match the real diamond band width. $a_{l\sigma}^{\dagger}$ and $a_{l\sigma}$ are the creation and annihilation operators of an electron with spin σ at site l. The electrons can hop only between the nearest neighboring sites expressed by $\langle l,l'\rangle$. μ stands for the chemical potential of electrons, and Δ_e is the potential difference after and before the substitution at the doped sites labeled by l_0. This parameter determines the formation and the position of the impurity band, i.e., the activation gap. It is determined according to the experimental value of about 0.37 eV. Q_l is the dimensionless coordinate operator of the phonon at site l, with a frequency ω_0. S denotes the e-ph coupling constant. $\bar{n}_l$ is the average electron number at site l. To simplify the problem, we just consider the coupling at the doped sites hereafter, because in pure diamond, there is no evidence that the phonon satellite structure appears. It implies that the coupling becomes important just after the doping, as discussed in Refs. 5 and 15. The doped boron atoms will introduce a strong coupling between the localized vibrational modes and electrons at around the Fermi surface of the BDD. There is also an experimental confirmation of this favored coupling in Ref. 20.

By using the Trotter decoupling formula and inserting the phonon eigenstate $|x_{l_0}\rangle$ of the operator Q_{l_0} by $Q_{l_0}|x_{l_0}\rangle=x_{l_0}|x_{l_0}\rangle$, the Boltzmann operator can be written in a path-integral form as[13]

$$e^{-\theta H}\rightarrow\int\mathcal{D}x\left[T_+\exp\left(-\int_0^{\theta}d\tau[h(\tau,x)+\Omega(\tau,x)]\right)\prod_{l_0}[|x_{l_0}(\theta)\rangle\langle x_{l_0}(0)|]\right], \tag{2}$$

where $\theta\equiv 1/k_BT$, T is the temperature, and

$$h(\tau,x)\equiv -t\sum_{\langle l,l'\rangle}\sum_{\sigma}[a_{l\sigma}^{\dagger}(\tau)a_{l'\sigma}(\tau)+a_{l'\sigma}^{\dagger}(\tau)a_{l\sigma}(\tau)] - \mu\sum_{l,\sigma}n_{l\sigma}(\tau)+\sum_{l_0,\sigma}n_{l_0\sigma}(\tau)[\Delta_e+S^2\bar{n}_{l_0}/\omega_0-Sx_{l_0}(\tau)], \tag{3}$$

$$\Omega(\tau,x)\equiv\sum_{l_0}\left[Sx_{l_0}(\tau)\bar{n}_{l_0}+\frac{1}{2\omega_0}\left(\frac{\partial x_{l_0}(\tau)}{\partial\tau}\right)^2+\frac{1}{2}\omega_0x_{l_0}^2(\tau)\right]. \tag{4}$$

We should note that the electronic operators $a_{l\sigma}(\tau)$, $n_{l\sigma}(\tau)$ have no real time dependence. The time argument τ only denotes the time ordering operated by T_+. While $x_{l_0}(\tau)$ is a time dependent c number. $\int\mathcal{D}x$ means the summation over all possible paths.

We define a time evolution matrix $\mathbf{R}(\tau,x)$ along a path x as

$$\mathbf{R}(\tau,x)\equiv T_+\exp\left(-\int_0^{\tau}d\tau'\mathbf{H}[\tau',x(\tau')]\right), \tag{5}$$

where

$$[\mathbf{H}(\tau,x)]_{jj'}\equiv\langle 0|a_j(\tau)h(\tau,x)a_{j'}^{\dagger}(\tau)|0\rangle. \tag{6}$$

j symbolically stands for site l and spin σ, and $|0\rangle$ means the true electron vacuum. The one-body Green's function of a given path x is defined as

$$G(j\tau,j'\tau',x)=-\text{sign}(\tau-\tau')\langle T_+\vec{a}_j(\tau)\vec{a}_{j'}^{\dagger}(\tau')\rangle_x, \tag{7}$$

which can be derived as

$$G(j\tau,j'\tau',x)=\left[\mathbf{R}(\tau,x)\begin{pmatrix}-\frac{1}{1+\mathbf{R}(\theta,x)}, & \tau>\tau'\\ \frac{1}{1+\mathbf{R}^{-1}(\theta,x)}, & \tau<\tau'\end{pmatrix}\mathbf{R}(\tau',x)\right]_{jj'}. \tag{8}$$

In Eq. (7), the operator $\vec{a}_j(\tau)$ is the Heisenberg representation of a_j, and is really time dependent. After the path integral, the ordinary Green's function [$\equiv G(ll',\tau)$] is obtained as

$$G(ll',\tau) = \int \mathcal{D}x e^{-\theta[\Phi(x)-\Phi]} G(l\tau,l'0,x). \tag{9}$$

Here, $\Phi(x)$ and Φ are the free energy along a given path x and the total free energy, respectively. This Green's function is site dependent obviously.

In the numerical calculation, the path integral of Eq. (9) is performed by the quantum Monte Carlo (QMC) simulation with a path updating method similar to Ref. 21, which is much more rapid and efficient than the standard Metropolis algorithm. To avoid numerical errors, we have employed a matrix factorization algorithm[22] with quad precision. Since the starting phonon configuration is generated randomly, it is necessary to take enough extra QMC sweeps to reach the system thermal equilibrium before measuring the electron number or the Green's function. Furthermore, in order to reduce the correlation between the consecutive measurements, we set an interval of adequate sweeps. In the QMC, the chemical potential μ is first determined by checking the electron number.

Because of the broken translational symmetry of this disordered system, we cannot use Fourier transformation to get the momentum dependent Green's functions or the Green's function corresponding to the total density of state (DOS) by a summation over the momenta. Nevertheless, we can make use of the invariance of representation transformation to sum up the one-body Green's function $G(ll',\tau)$ over sites as

$$G(\tau) = \frac{1}{N}\sum_{l} G(ll,\tau). \tag{10}$$

Then the spectral function $A(\omega)$ can be derived through the analytic continuation as

$$G(\tau) = -\int_{-\infty}^{+\infty} \frac{e^{-\tau\omega}}{1+e^{-\theta\omega}} A(\omega)d\omega, \tag{11}$$

which is carried out here by an iterative fitting method introduced in Ref. 16. Here, we should mention that in Eq. (10), N can be either the total system size or a part of it, such as all the doped sites, depending on the site l we choose. That is to say, we can calculate different spectra by selecting different l, which will be shown and discussed in detail later. Finally, the PES intensity function $I(\omega)$ is calculated as $I(\omega) = A(\omega)f(\omega)$ by imposing the Fermi distribution $f(\omega)$ to compare with the experimental results, since the PES experiment only detects the occupied electronic states.

III. RESULTS AND DISCUSSIONS

Because we take into account the e-ph coupling only at those doped sites, the phonon effect is not so clear in the whole system spectrum after averaging over all sites. To clarify the phonon quantum effect, we shall also present the spectral intensity of doped sites.

First, as a reference, we compute the spectra for the simple cubic lattice of different doping rates by the classical Monte Carlo (CMC) simulation[23] as shown in Fig. 1, wherein the kinetic energy of the phonon is neglected and the one-body Green's function is obtained by directly diagonalizing the electronic Hamiltonian. The system size is $8\times8\times8$, and the parameters are $\omega_0=0.25$ eV, $S=0.25$ eV, and $\theta=14.4$ eV^{-1}. Correspondingly, the dimensionless coupling constant λ ($\equiv\frac{S^2}{2d\omega_0 t}$, where d is the dimension) is 0.1. From the whole system spectra (solid lines), we can clearly see the emergence of a Fermi edge on increasing the doping percentage. In the low doping case, the impurity levels are a little above the top of the valence band, and the material is a semiconductor with a small activation gap. In the higher doping case, the impurity band expands up to the top of the valence band, and the gap is filled up. Thus, the sample undergoes a semiconductor-metal transition, and the electrons can move freely from one impurity atom to another by tunneling through the intermediate carbon atoms. As for the spectra of doped sites (dashed lines), apart from the main impurity band, there is a long tail extending almost over the valence band. This is due to the modification of impurity levels by an admixture of the continuum valence band, as described by the Fano effect.[24] This effect is also exhibited in Ref. 22 by using a static single-impurity model to explain the origin of the multipeak spectra.

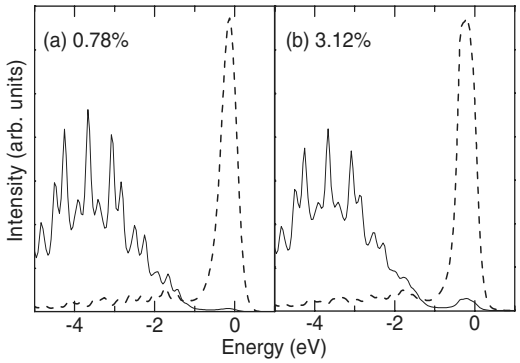

FIG. 1. The spectra for the simple cubic lattice of different doping rates by the QMC. The zero is the position of the Fermi level. Dotted lines and solid ones denote the spectra of doped sites and the whole system, respectively.

In Fig. 2, we calculate the spectra for the simple cubic lattice of different doping rates by the QMC method, which is free from the approximation used in the previous CMC. The parameters are the same as in Fig. 1. Since the system size is small, $4\times4\times4$, the value of the doping rate seems to be relatively high, but the absolute number of the doped sites is small. In the whole system spectra (solid lines), the semiconductor-metal phase transition is reproduced completely with the increase of doping rate. In order to illustrate the different contributions to the DOS from doped atoms and undoped atoms, the undoped site spectrum (dashed line) and the whole system spectrum (solid line) near the Fermi level are shown as an inset in Fig. 2(c). It is obvious that the disordered states in the PES make the activation gap smaller.

In Fig. 2, for the doped site spectra (dashed lines), a phonon satellite structure is clearly seen in each panel, lying a little below the Fermi level, in addition to the aforementioned Fano tail. This side structure has not been found in the classical cases, and obviously comes from the phonon quantum property in the e-ph coupling, while its shape is should-

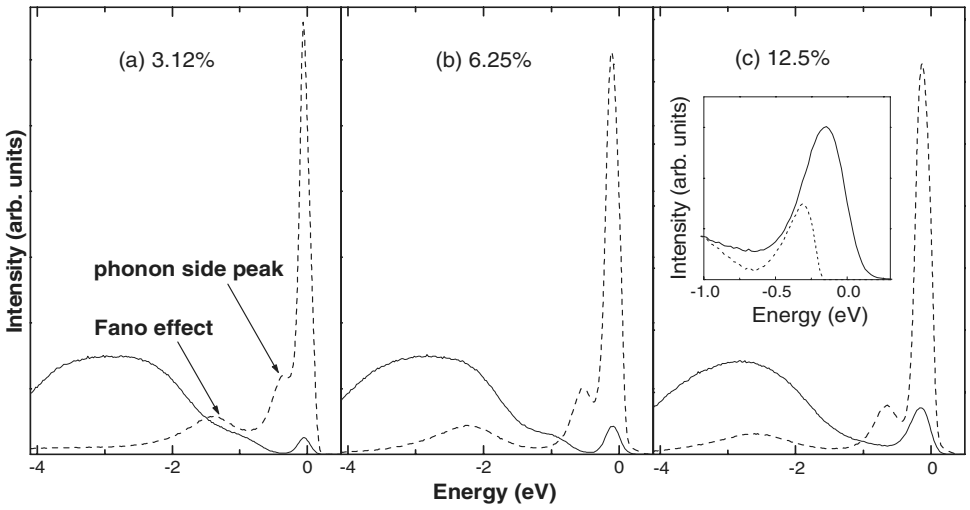

FIG. 2. The spectra for the simple cubic lattice of different doping rates by the QMC. The zero is the position of the Fermi level. Dotted lines and solid ones denote the spectra of doped sites and the whole system, respectively. The inset in (c) is the whole system spectrum (solid curve) and the undoped site spectrum (dashed curve) near the Fermi level.

erlike instead of the δ-function-like peaks given in the localized electron model.[11] Actually, in our QMC simulations, we have used several different values of phonon frequency between 0.10 and 0.30 eV. The phonon structures are observed in all these cases, but most clearly when $\omega_0 \geqslant 0.25$ eV, due to low resolution and temperature limitation of the QMC approach. Although we show only the results of $\omega_0=0.25$ eV here, we believe the physical essence of the steplike satellite structure is already captured through this calculation.

We should note that in the three panels of Fig. 2, the positions of the phonon side peaks (dashed lines), 0.3 eV in (a), 0.5 eV in (b), and 0.6 eV in (c), are a little different from the ones expected from the phonon frequency we have used ($\omega_0=0.25$ eV). As discussed in Refs. 16 and 25, the PES of a uniform system is determined by the simultaneous momentum and energy conservation of the e-ph system. The energy interval ($\equiv\Delta\varepsilon$) between the zero-phonon (no e-ph scattering) peak and the single-phonon one is dependent not only on the phonon frequency but also on the electron energy band by the formula $\Delta\varepsilon=(\varepsilon_{p+q}+\omega_{-q})-\varepsilon_p$, where ε_p denotes the energy of an original photoemitted electron with momentum p. It changes to $\varepsilon_{p+q}+\omega_{-q}$ after emitting a phonon of momentum $-q$. The localized electron model is a special case, wherein the electron is pinned at one site. Thus, the self-scattering process guarantees that the interval is decided only by the phonon frequency. Using Einstein phonons, it is naturally of an equal interval. As for the present model, it bears similarities to the above two cases, as denoted in the Hamiltonian. In the low doping rate case such as Fig. 2(a), the impurity levels are few or the impurity band is very shallow, which is similar to the localized electron case, then the interval between the zero-phonon peak and the single-phonon peak is almost equal to the Einstein phonon frequency. In heavily doped samples such as shown in Figs. 2(b) and 2(c), the impurity band expands and its shape plays greater roles, then the side structure appears to be much wider and irregular in position. At the same time, this single-phonon peak is also modified by the impurity band to shift a little from the original position of 0.25 eV and become asymmetric according to the aforementioned Fano effect. When combined together, it presents as a shoulderlike shape in the doped site spectra, with irregular energy intervals, even within the Einstein phonon model.

Obviously, the e-ph coupling also greatly contributes to the expansion of the impurity band and the filling of the activation gap. As shown in Fig. 2, the phonon side structure lies a little below the Fermi level, at the very scope of the semiconductor gap. If the e-ph effect is strong or the doping rate is high, this side structure expansion in the doped site spectra can contribute much to the whole system spectra. In Fig. 3, we give the spectra of a low doping rate, same as Fig. 2(a), but increasing the coupling constant to 0.5 eV instead of $S=0.25$ eV used in Figs. 1 and 2. Then, the λ is 0.4. Comparing with Fig. 2(a), the strong coupling between the electrons and the phonons not only greatly intensifies the single-phonon peak, but also arouses double-phonon or even multiphonon scattering processes, because another shoulder appears clearly besides the investigated single-phonon one and the Fano tail in the doped sites spectrum (dashed line). Thus, the localization character of electrons is exhibited incisively and vividly. As discussed above, this effect can expand the impurity band to fill the gap, thus making the phase transition occur, as shown clearly in the whole system spec-

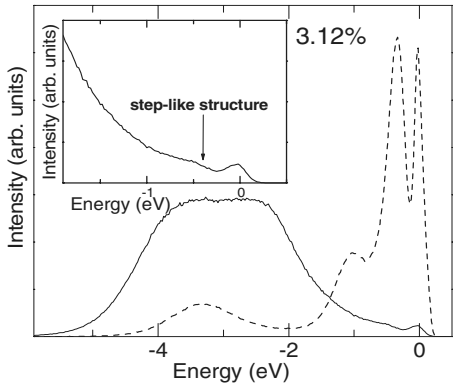

FIG. 3. The spectra for doped simple cubic lattice with an intermediate e-ph coupling. The zero is the position of the Fermi level. The dotted (solid) line is the spectrum of doped sites (the whole system). The inset is a zoom in on the solid line near the Fermi level.

trum (solid line). Though obscure, we can even affirm the steplike shape in the whole system spectrum, which locates at the very position of the single-phonon peak in the doped site spectra. The region near the Fermi level is zoomed in at the inset. From this figure, we can see clearly the coexistence of a Fermi edge and the steplike multiphonon satellite structure.

The multiphonon process can be clearly seen only in the larger S case. While in the small S case, only the single-phonon process can be observed. So, we just pick two typical S cases (weak one and intermediate one) for this paper. They are enough to clarify the physics and the experiment.

As mentioned, the path-integral theory we used here has one more advantage over the CPA. It can distinguish the different components in the material as we have done in calculating the spectra of doped and undoped sites. In reality, this differentiation can be achieved by the resonance PES[25] experiments. Tuning the incident photon energy to stimulate the atom core-level absorption excitation, the possible immediate Auger decay emits an electron, which can interfere with a directly photoemitted valence band electron. The overlap of these two electrons can be described as a function of the incident photon energy by the so-called Fano line shape.[24] For the material BDD, the excitation energy of carbon core-level 1S to the top of the valence band is about 284 eV, much different from that of boron, which is about 190 eV. Therefore, by sweeping the photon energy from low values through the above values, the spectrum reflecting the boron atom core-level absorption can be observed first, and then the carbon atoms; thus, the different components are identified.

IV. CONCLUSION

In summary, we have calculated the PES of the doped simple cubic lattice by applying a path-integral theory to the many-impurity Holstein model to reproduce the coexistence of a Fermi edge and the multiphonon satellite structure, which embodies the coexistence of the two intrinsic attributes of electrons: itineracy and localization. The one-body lattice Green's function is calculated by the QMC method to derive the spectral function. Due to the e-ph coupling and the increase of dopant concentration, the impurity band extends up to the top of the valence band, and then fills the semiconductor gap gradually. The semiconductor-metal transition takes place. Thus, the electrons can itinerate from one impurity atom to another one through those intermediate carbon atoms. At the same time, the coupling between electrons and Einstein phonons induces the multiphonon steplike satellite structure, indicating the localization of the electrons by Einstein phonons. Though using a simple lattice structure, our theoretical interpretation is quite important to clarify the coexistence of a Fermi edge and the steplike satellite structure detected in the PES of the BDD. Since silicon has a similar lattice structure to diamond, and the doping with boron is also substitutional,[26] these characteristics are also expected in boron-doped silicon, in which the SC is discovered recently.[26]

ACKNOWLEDGMENT

This work was supported by the next generation of supercomputing project, Nanoscience program, MEXT, Japan.

[1] E. A. Ekimov, V. A. Sidorov, E. D. Bauer, N. N. Mel'nik, N. J. Curro, J. D. Thompson, and S. M. Stishov, Nature (London) **428**, 542 (2004).
[2] L. Boeri, J. Kortus, and O. K. Andersen, Phys. Rev. Lett. **93**, 237002 (2004).
[3] K. W. Lee and W. E. Pickett, Phys. Rev. Lett. **93**, 237003 (2004).
[4] Y. Ma, J. S. Tse, T. Cui, D. D. Klug, L. Zhang, Y. Xie, Y. Niu, and G. Zou, Phys. Rev. B **72**, 014306 (2005).
[5] X. Blase, Ch. Adessi, and D. Connétable, Phys. Rev. Lett. **93**, 237004 (2004).
[6] A. T. Collins and A. W. S. Williams, J. Phys. C **4**, 1789 (1971).
[7] E. Bustarret, J. Kačmarčik, C. Marcenat, E. Gheeraert, C. Cytermann, J. Marcus, and T. Klein, Phys. Rev. Lett. **93**, 237005 (2004).
[8] Y. Takano, M. Nagao, T. Takenouchi, H. Umezawa, I. Sakaguchi, M. Tachiki, and H. Kawarada, Diamond Relat. Mater. **14**, 1936 (2005).
[9] K. Ishizaka, R. Eguchi, S. Tsuda, T. Kiss, T. Shimojima, T. Yokoya, S. Shin, T. Togashi, S. Watanabe, C.-T. Chen, C. Q. Zhang, Y. Takano, M. Nagao, I. Sakaguchi, T. Takenouchi, and H. Kawarada, Sci. Technol. Adv. Mater. **7**, S17 (2006).
[10] F. Giustino, J. R. Yates, I. Souza, M. L. Cohen, and G. Louie, Phys. Rev. Lett. **98**, 047005 (2007).
[11] G. D. Mahan, *Many-Particle Physics*, 3rd ed. (Plenum, New York, 2000), Chap. 4.
[12] P. Soven, Phys. Rev. **156**, 809 (1967).
[13] K. Nasu, J. Phys. Soc. Jpn. **65**, 2285 (1996).
[14] T. Holstein, Ann. Phys. (N.Y.) **8**, 325 (1959).
[15] H. J. Xiang, Z. Li, J. Yang, J. G. Hou, and Q. Zhu, Phys. Rev. B **70**, 212504 (2004).
[16] K. Ji, H. Zheng, and K. Nasu, Phys. Rev. B **70**, 085110 (2004).
[17] S. Kumar and P. Majumdar, Phys. Rev. Lett. **94**, 136601 (2005).
[18] F. X. Bronold, A. Saxena, and A. R. Bishop, Phys. Rev. B **63**, 235109 (2001).
[19] S. Ciuchi, F. de Pasquale, S. Fratini, and D. Feinberg, Phys. Rev. B **56**, 4494 (1997).
[20] M. Ortolani, S. Lupi, L. Baldassarre, U. Schade, P. Calvani, Y. Takano, M. Nagao, T. Takenouchi, and H. Kawarada, Phys. Rev. Lett. **97**, 097002 (2006).
[21] R. Blankenbecler, D. J. Scalapino, and R. L. Sugar, Phys. Rev. D **24**, 2278 (1981).
[22] M. Yamazaki, N. Tomita, and K. Nasu, J. Phys. Soc. Jpn. **72**, 611 (2003).
[23] J. Han, K. Ji, Z. Zhu, and K. Nasu, Phys. Rev. B **73**, 125111 (2006).
[24] U. Fano, Phys. Rev. **124**, 1866 (1961).
[25] F. Reinert and S. Hüfner, New J. Phys. **7**, 97 (2005).
[26] E. Bustarret, C. Marcenat, P. Achatz, J. Kačmarčik, F. Lévy, A. Huxley, L. Ortéga, E. Bourgeois, X. Blase, D. Débarre, and J. Boulmer, Nature (London) **444**, 465 (2006).